

# The isotopic signature of U<sup>V</sup> during bacterial reduction

**A.R. Brown, M. Molinas, Y. Roebbert, R. Faizova, T. Vitova, A. Sato, M. Hada, M. Abe, M. Mazzanti, S. Weyer, R. Bernier-Latmani**

## Supplementary Information

The Supplementary Information includes:

- Experimental Section
- Figures S-1 to S-3
- Table S-1
- Supplementary Information References

## Experimental Section

### Synthesis of natural U<sup>VI</sup>-dpaea

Solid phase U<sup>VI</sup>O<sub>2</sub>-dpaea was synthesised as described previously (Faizova *et al.*, 2018). Briefly, natural U from an IRMM-184 nitrate stock was reacted with H<sub>2</sub>dpaea in methanol and then evaporated to dryness. The powder was then transferred to an anoxic chamber (100% N<sub>2</sub>, <0.1 ppm O<sub>2</sub>; MBraun, Germany) and stored in the dark.

### Cultivation of *Shewanella oneidensis*

To follow the reduction and fractionation of U<sup>VI</sup>-dpaea, a high biomass inoculum of *Shewanella oneidensis* MR-1 was obtained by first growing it in oxic Luria-Bertani (LB) medium to mid-late exponential phase. The biomass was harvested by centrifugation for 10 min at 5000×g and was washed three times in an anoxic and sterile buffer that was modified from a Widdel low phosphate (WLP) medium to exclude carbonate and phosphate as potential U complexing agents. The composition was as follows: 0.68 mM CaCl<sub>2</sub>·2H<sub>2</sub>O, 6.71 mM KCl, 2.46 MgCl<sub>2</sub>·6H<sub>2</sub>O, 85.56 mM NaCl, 4.67 mM NH<sub>4</sub>Cl 4.67 and 20 mM piperazine-N,N'-bis(2-ethanesulfonic acid) (PIPES) at pH 7.3.

### Reduction of U<sup>VI</sup>-dpaea by *S. oneidensis*

U<sup>VI</sup>-dpaea reduction was followed under non-growth conditions with 20 mM sodium lactate serving as the electron donor. Here, aliquots of the washed cell suspension were added to anoxic and sterile reactors containing the modified WLP medium and ~130 μM U (equivalent aqueous concentration) as solid phase U<sup>VI</sup>-dpaea powder. U reduction experiments were performed in two batches. The first was performed as a series of sacrificial reactors, allowing all the U oxidation states (solid U<sup>VI</sup>, aqueous U<sup>V</sup> and solid U<sup>IV</sup>) to be successfully separated and quantified by anion exchange chromatography (see below). The aqueous U was separated from the solid phase by centrifugation at 12000×g for 10



min, followed by filtration of the supernatant through 0.22  $\mu\text{m}$  PTFE filters. The solid phase was then acidified in 6 N HCl and immediately added to anion exchange columns for separation of  $\text{U}^{\text{VI}}$  and  $\text{U}^{\text{IV}}$  oxidation states. The second batch was performed in duplicate reactors and only the aqueous U was separated and quantified, in order to confirm the findings of the first sacrificial reactor batch experiment.

### Anion exchange chromatography

In order to quantify  $\text{U}^{\text{VI}}$  reduction and isotope signatures over time in all experiments,  $\text{U}^{\text{VI}}$  was separated from total U using an anion exchange chromatography protocol adapted from Stoliker *et al.* (Stoliker *et al.*, 2013a, 2013b) and used previously (Molinas *et al.*, 2021, 2023). Briefly, strongly basic anion exchange resin (Dowex 1X8; 100–200 mesh) was added to polypropylene chromatographic columns to a bed volume of 2.5 mL. The resin was then preconditioned with 4.5 N HCl prior to addition of a U-containing sample that had been acidified to 4.5 N HCl. First, the  $\text{U}^{\text{IV}}$  fraction was eluted with 10 consecutive bed volumes of 4.5 N HCl, followed by elution of  $\text{U}^{\text{VI}}$  with 10 bed volumes of 0.1 N HCl. All steps were performed inside an anoxic chamber with Ultra-pure reagents that were flushed with nitrogen for more than 2 h before use. After separation, U concentrations in each fraction were quantified using ICP-MS. Previous studies observed isotopic cross-contamination between the two U oxidation states and thus applied a correction factor to the measured  $\delta^{238}\text{U}$  (Wang *et al.*, 2015a, 2015b). However, our own tests, using the conditions above, showed negligible cross-contamination and no correction factor was required.

### U isotope ratio analysis

Sample preparation for U isotope measurements were performed as described previously (Brown *et al.*, 2023), except that, prior to purification on Eichrom UTEVA resins, a weighed aliquot of the  $^{236}\text{U}/^{233}\text{U}$  double spike solution (IRMM 3636-A,  $^{236}\text{U}/^{233}\text{U} = 0.98130$ ) was added to the samples in order to correct for isotope fractionation during U purification and instrumental mass discrimination during MC-ICP-MS analysis (Richter *et al.*, 2008; Weyer *et al.*, 2008). Spike/sample mixtures for all samples and standards were adjusted to similar ratios ( $^{236}\text{U}/^{235}\text{U} \approx 3 \pm 10\%$ ) to minimize peak tailing effects (from the ion beams of  $^{238}\text{U}$  on  $^{236}\text{U}$  and of  $^{236}\text{U}$  on  $^{235}\text{U}$ ).

For sample analysis, two sample measurements were bracketed by two standard measurements and all samples and standards were measured with  $\sim 4$  min total integration time. Mass bias correction was performed with the IRMM 3636 double spike (Richter *et al.*, 2008) and the exponential law (Russell *et al.*, 1978).

As before, isotope signatures are presented in the delta notation relative to the IRMM-184 U standard:

$$\delta^{238}\text{U} = \left[ \frac{(^{238}\text{U}/^{235}\text{U})_{\text{sample}}}{(^{238}\text{U}/^{235}\text{U})_{\text{standard}}} - 1 \right] \cdot 1000 \quad [\text{‰}] \quad (\text{Eq. S-1})$$

### Rayleigh distillation models

Rayleigh distillation models were used to determine isotope fractionation factors ( $\epsilon$ ) using the method described previously (Brown *et al.*, 2023; Scott *et al.*, 2004).

### *Ab initio* calculation of $\epsilon^{\text{eq}}$ between $\text{U}^{\text{VI}}$ and $\text{U}^{\text{IV}}$

We modelled the  $\text{U}^{\text{VI}}$  and  $\text{U}^{\text{V}}$  species as the dpaea complexes  $\text{UO}_2\text{-dpaea}$  and  $\text{UO}_2\text{-dpaea}^-$ , respectively, using the structures reported previously (Faizova *et al.*, 2018). The  $\text{U}^{\text{IV}}$  product was modelled as either  $\text{U}^{\text{IV}}\text{-}(\text{dpaea})_2$  or a non-uraninite  $\text{U}^{\text{IV}}$  species, the two likely products of this biological reaction (Molinas *et al.*, 2021). The non-uraninite  $\text{U}^{\text{IV}}$



was modelled as a cluster of ningyoite ( $\text{H}_2\text{6CaU}(\text{PO}_4)_{10}^{2+}$ ), as established previously (Sato *et al.*, 2021), which is a close analogue of the non-crystalline biotic reduction products (Alessi *et al.*, 2014; Bernier-Latmani *et al.*, 2010; Sato *et al.*, 2021).

Calculations were performed as described previously (Brown *et al.*, 2023). The nuclear mass term,  $\ln K_{\text{nm}}$ , was calculated as a difference in the logarithms of the reduced partition function ratio,  $\beta$ , of  $\text{U}^{\text{IV}}$ ,  $\text{U}^{\text{V}}$  and  $\text{U}^{\text{VI}}$ , e.g.:

$$\ln K_{\text{nm}} = \ln \beta(\text{U}^{\text{V}}) - \ln \beta(\text{U}^{\text{VI}}) \quad (\text{Eq. S-2})$$

### U M<sub>4</sub>-edge HR-XANES spectroscopy

U M<sub>4</sub>-edge HR-XANES spectra were recorded at the station for actinide science (ACT) at the CAT-ACT beamline at the Karlsruhe Research Accelerator (KARA), Karlsruhe, Germany, which is equipped with a Johann type X-ray emission spectrometer (Zimina *et al.*, 2017). Spectra were collected as described previously (Molinas *et al.*, 2021), and data processing and normalisation was performed using the ATHENA software (Ravel and Newville, 2005).

### Equilibrium isotope exchange between U<sup>V</sup>-dpaea and the U<sup>IV</sup> product

Abiotic equilibrium isotope exchange between U<sup>V</sup> and U<sup>IV</sup> was determined during the reaction between ~110 μM U<sup>V</sup>-dpaea with an initial isotopic composition of ~5‰, and ~57 μM U<sup>IV</sup> present as the product of the bioreduction experiments of natural U, with an initial isotopic composition of 0‰. The U speciation was maintained using the same medium composition as for bioreduction experiments. Bacterial cells were inactivated via sonication to ensure no further biologically-mediated redox change. Samples were filtered through 0.22 μm filters and U concentrations and isotope signatures were determined by ICP-MS and MC-ICP-MS, respectively.



## Supplementary Figures

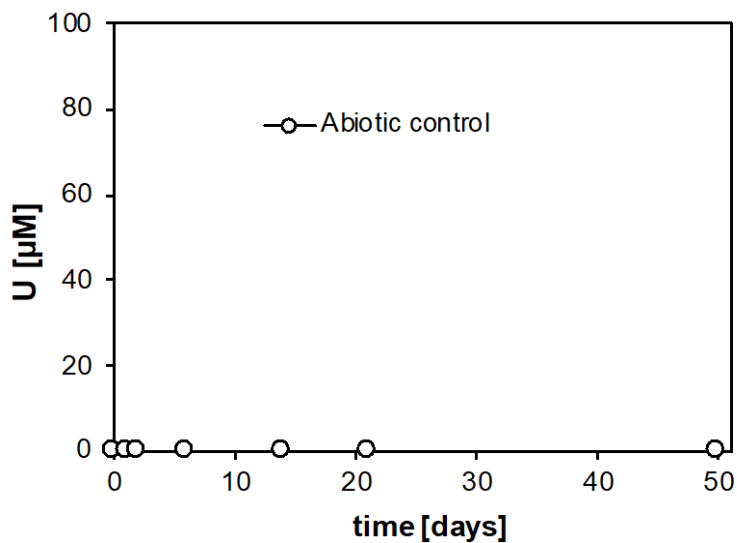


**Figure S-1** Aqueous uranium concentrations in abiotic control experiments. Samples were filtered through 0.22 µm filters. Symbols depict the mean of duplicate reactors and error bars show 1 standard deviation of the mean. Where not visible, the error is smaller than the symbol size.

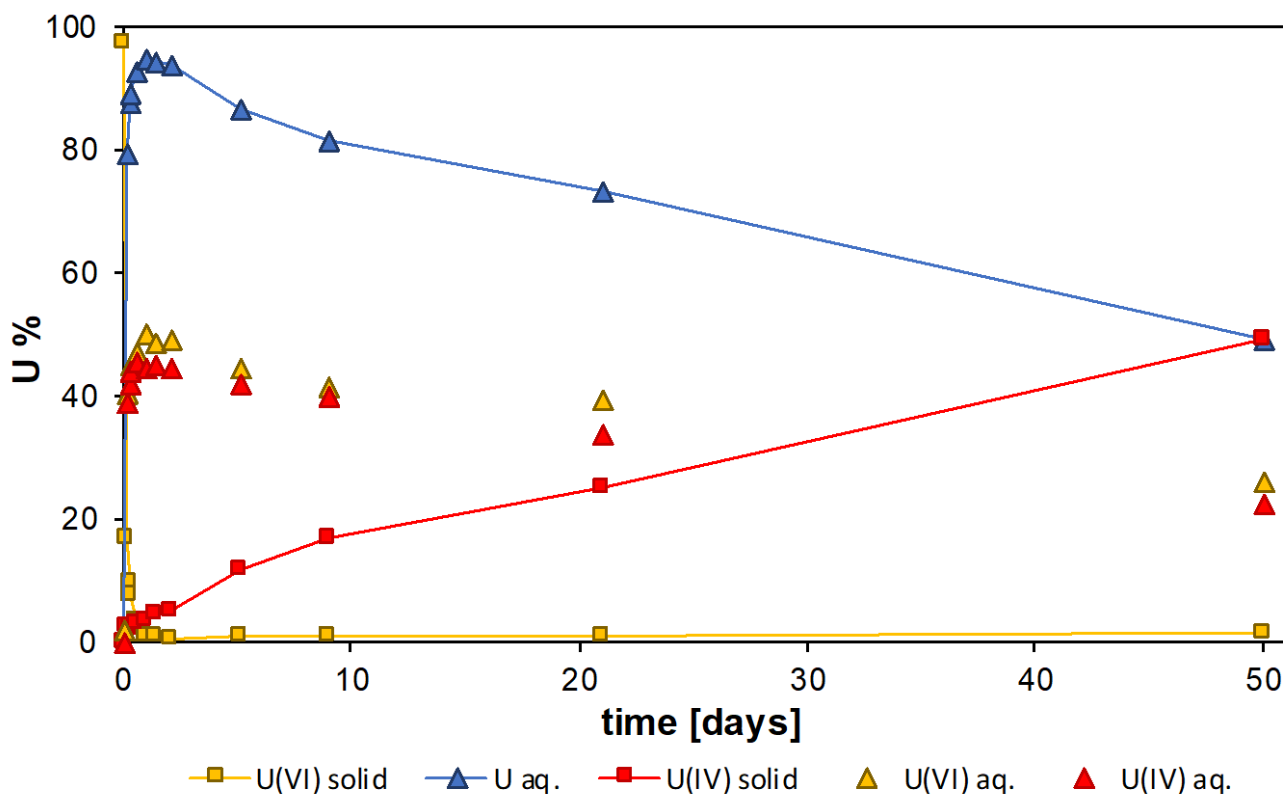


**Figure S-2** Uranium mass distribution in a series of sacrificial reactors. The aqueous uranium (blue triangles) was acidified with 4.5 N HCl and immediately underwent anion exchange chromatography to quantitatively separate  $U^{IV}$  (red triangles) and  $U^{VI}$  (yellow triangles). The  $\delta^{238}U$  values of each valence state of the 48-h sample were  $-0.04 \pm 0.04$  ‰ and  $0.03 \pm 0.02$  ‰, respectively.



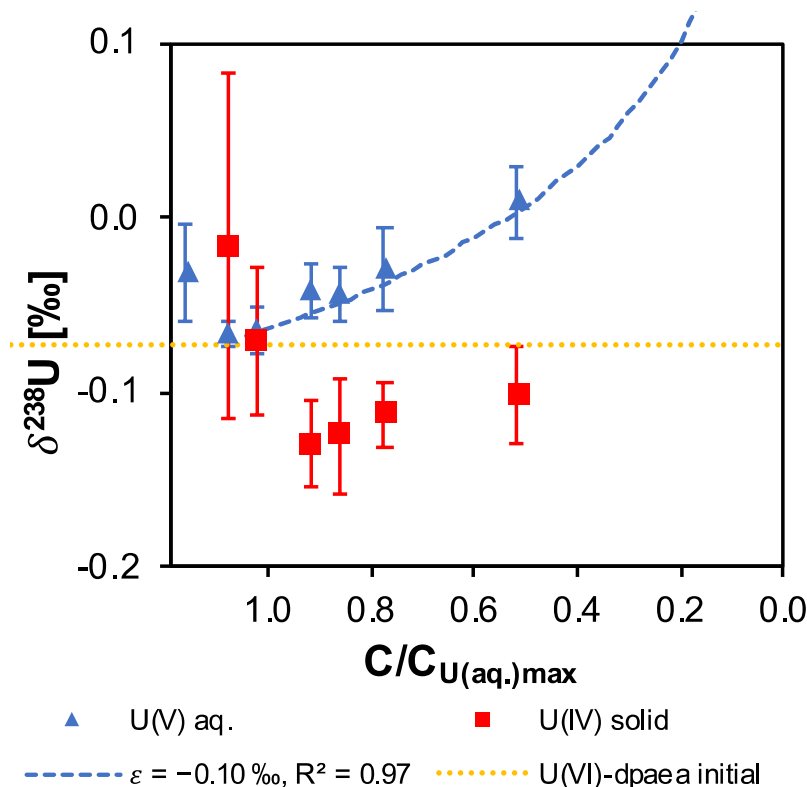


**Figure S-3**  $\delta^{238}\text{U}$  values for each of the U components as a function of the aqueous  $\text{U}^{\text{V}}$  concentration, reported as a fraction of the maximum  $\text{U}^{\text{V}}$  concentration. These data correspond to the concentration data reported in Figure 1a. Symbols and error bars depict two standard deviations of the mean of triplicate measurements. The Rayleigh model (blue dashed line) of the  $\delta^{238}\text{U}$  values of  $\text{U}^{\text{V}}$  correspond to the linear best fit of the logarithmic data,  $R^2 = 0.97$ , from which the isotope enrichment factor,  $\epsilon$ , is derived. The  $\delta^{238}\text{U}$  value of the initial  $\text{U}^{\text{VI}}$ -dpaea is plotted as a yellow dotted line.

## Supplementary Table

**Table S-1**  $\ln K_{\text{fs}}$  (nuclear field shift effect term),  $\ln K_{\text{nm}}$  (nuclear mass term) and  $\epsilon^{\text{eq}}$  (total fractionation factor) for the reduction of  $\text{U}^{\text{VI}}$  to  $\text{U}^{\text{V}}$  and that of  $\text{U}^{\text{V}}$  to  $\text{U}^{\text{IV}}$ .  $\ln K_{\text{fs}}$  was calculated by either X2C-Hartree-Fock (X2C-HF) or X2C-B3LYP, and the values are shown in the columns of “HF” and “B3LYP”, respectively. Likewise, the total fractionation factor is shown for both calculation methods of  $\ln K_{\text{fs}}$ . All values are shown in units of ‰ (permil). The computational methods are described above.

Reaction	$\ln K_{\text{fs}}$		$\ln K_{\text{nm}}$	$\epsilon^{\text{eq}}$	
	HF	B3LYP		HF	B3LYP
$\text{U}^{\text{VI}}\text{O}_2\text{-dpaea} \rightarrow \text{U}^{\text{V}}\text{O}_2\text{-dpaea}^-$	1.98	1.21	-0.39	1.60	0.82
$\text{U}^{\text{V}}\text{O}_2\text{-dpaea}^- \rightarrow \text{U}^{\text{IV}}\text{-(dpaea)}_2$	0.96	1.01	-0.68	0.27	0.33
$\text{U}^{\text{V}}\text{O}_2\text{-dpaea}^- \rightarrow \text{CaU}^{\text{IV}}(\text{PO}_4)_2$	1.04	0.71	-0.58	0.46	0.13



## Supplementary Information References

- Alessi, D.S., Lezama-Pacheco, J.S., Stubbs, J.E., Janousch, M., Bargar, J.R., Persson, P., Bernier-Latmani, R. (2014) The product of microbial uranium reduction includes multiple species with U(IV)-phosphate coordination. *Geochimica et Cosmochimica Acta* 131, 115–127. <https://doi.org/10.1016/j.gca.2014.01.005>
- Bernier-Latmani, R., Veeramani, H., Vecchia, E.D., Junier, P., Lezama-Pacheco, J.S., Suvorova, E.I., Sharp, J.O., Wigginton, N.S., Bargar, J.R. (2010) Non-uraninite products of microbial U (VI) reduction. *Environmental Science and Technology* 44, 9456–9462. <https://doi.org/10.1021/es101675a>
- Brown, A.R., Roebbert, Y., Sato, A., Hada, M., Abe, M., Weyer, S., Bernier-Latmani, R. (2023) Contribution of the nuclear field shift to kinetic uranium isotope fractionation. *Geochemical Perspectives Letters* 27, 43–47. <https://doi.org/10.7185/geochemlet.2333>
- Faizova, R., Scopelliti, R., Chauvin, A.-S., Mazzanti, M. (2018) Synthesis and characterization of a water stable uranyl(V) complex. *Journal of the American Chemical Society* 140, 13554–13557. <https://doi.org/10.1021/jacs.8b07885>
- Molinas, M., Faizova, R., Brown, A., Galanzew, J., Schacherl, B., Bartova, B., Meibom, K.L., Vitova, T., Mazzanti, M. and Bernier-Latmani, R. (2021) Biological reduction of a U(V)-organic ligand complex. *Environmental Science and Technology* 55, 4753–4761. <https://doi.org/10.1021/acs.est.0c06633>
- Molinas, M., Meibom, K.L., Faizova, R., Mazzanti, M., Bernier-Latmani, R. (2023) Mechanism of reduction of aqueous U(V)-dopa and solid-phase U(VI)-dopa complexes: The role of multiheme *c*-type cytochromes. *Environmental Science and Technology* 57, 7537–7546. <https://doi.org/10.1021/acs.est.3c00666>
- Ravel, B., Newville, M. (2005) ATHENA, ARTEMIS, HEPHAESTUS: Data analysis for X-ray absorption spectroscopy using IFEFFIT. *Journal of Synchrotron Radiation* 12, 537–541. <https://doi.org/10.1107/S0909049505012719>
- Richter, S., Alonso-Munoz, A., Eykens, R., Jacobsson, U., Kuehn, H., Verbruggen, A., Aregbe, Y., Wellum, R., Keegan, E. (2008) The isotopic composition of natural uranium samples—Measurements using the new  $n(^{233}\text{U})/n(^{236}\text{U})$  double spike IRMM-3636. *International Journal of Mass Spectrometry* 269, 145–148. <https://doi.org/10.1016/j.ijms.2007.09.012>
- Russell, W.A., Papanastassiou, D.A., Tombrello, T.A. (1978) Ca isotope fractionation on the Earth and other solar system materials. *Geochimica et Cosmochimica Acta* 42, 1075–1090. [https://doi.org/10.1016/0016-7037\(78\)90105-9](https://doi.org/10.1016/0016-7037(78)90105-9)
- Sato, A., Bernier-Latmani, R., Hada, M., Abe, M. (2021) *Ab initio* and steady-state models for uranium isotope fractionation in multi-step biotic and abiotic reduction. *Geochimica et Cosmochimica Acta* 307, 212–227. <https://doi.org/10.1016/j.gca.2021.05.044>
- Scott, K.M., Lu, X., Cavanaugh, C.M., Liu, J.S. (2004) Optimal methods for estimating kinetic isotope effects from different forms of the Rayleigh distillation equation. *Geochimica et Cosmochimica Acta* 68, 433–442. [https://doi.org/10.1016/S0016-7037\(03\)00459-9](https://doi.org/10.1016/S0016-7037(03)00459-9)
- Stoliker, D.L., Campbell, K.M., Fox, P.M., Singer, D.M., Kaviani, N., Carey, M., Peck, N.E., Bargar, J.R., Kent, D.B., Davis, J.A. (2013a) Evaluating chemical extraction techniques for the determination of uranium oxidation state in reduced aquifer sediments. *Environmental Science and Technology* 47, 9225–9232. <https://doi.org/10.1021/es401450v>
- Stoliker, D.L., Kaviani, N., Kent, D.B., Davis, J.A. (2013b) Evaluating ion exchange resin efficiency and oxidative capacity for the separation of uranium(IV) and uranium(VI). *Geochemical Transactions* 14, 1. <https://doi.org/10.1186/1467-4866-14-1>
- Wang, X., Johnson, T.M., Lundstrom, C.C. (2015a) Low temperature equilibrium isotope fractionation and isotope exchange kinetics between U(IV) and U(VI). *Geochimica et Cosmochimica Acta* 158, 262–275. <https://doi.org/10.1016/j.gca.2015.03.006>
- Wang, X., Johnson, T.M., Lundstrom, C.C. (2015b) Isotope fractionation during oxidation of tetravalent uranium by dissolved oxygen. *Geochimica et Cosmochimica Acta* 150, 160–170. <https://doi.org/10.1016/j.gca.2014.12.007>
- Weyer, S., Anbar, A.D., Gerdes, A., Gordon, G.W., Algeo, T.J., Boyle, E.A. (2008) Natural fractionation of  $^{238}\text{U}/^{235}\text{U}$ . *Geochimica et Cosmochimica Acta* 72, 345–359. <https://doi.org/10.1016/j.gca.2007.11.012>
- Zimina, A., Dardenne, K., Denecke, M.A., Doronkin, D.E., Huttel, E., Lichtenberg, H., Mangold, S., Pruessmann, T., Rothe, J., Spangenberg, T., Steininger, R., Vitova, T., Geckeis, H., Grunwaldt, J.D. (2017) CAT-ACT - A New Highly Versatile x-Ray Spectroscopy Beamline for Catalysis and Radionuclide Science at the KIT Synchrotron Light Facility ANKA. *Review of Scientific Instruments* 88, 113. <https://doi.org/10.1063/1.4999928>

